

Tunable doubly resonant optical parametric oscillator with LBO and KTP crystals pumped by second harmonic of a nanosecond Nd:YAG laser

R. DABU, C. FENIC, A. STRATAN, C. LUCULESCU

National Institute for Laser, Plasma and Radiation Physics, Laser Department, P.O. Box MG 36, Bucharest 76900, Romania.

L. MUSCALU

Prooptica, Bucovina Str. 4, 74404 Bucharest, Romania.

We compare two types of optical parametric oscillators (OPO's) with LBO and KTP crystals, pumped with a frequency doubled Q-switched Nd:YAG laser. The threshold pump power density near degeneracy was found to be 29 MW/cm² for the pulsed doubly resonant oscillator (DRO) with LBO, and 5.7 MW/cm² for the DRO with KTP. The DRO was continuously tuned in the near infrared by rotation of LBO and KTP crystals. The full width at half-maximum (FWHM) linewidth of the signal radiation emitted by DRO-LBO at 998 nm was 10 nm, and 0.65 nm for DRO-KTP at 1052.6 nm.

1. Introduction

The OPO's are very useful in producing tunable coherent radiation over wide ranges in the infrared, visible, and ultraviolet regions.

If a pump radiation with ω_p frequency is incident on a nonlinear material, then a signal ω_s frequency may be amplified. In the process, a third ω_i frequency, termed as the idler frequency, and such that $\omega_s + \omega_i = \omega_p$ is generated. In order to achieve significant parametric amplification it is required that at each of these frequencies the generated polarization travels at the same velocity as a freely propagating electromagnetic wave. This is the case when the refractive indices of the material are such that the wave vectors \mathbf{k} satisfy the momentum matching condition $\mathbf{k}_s + \mathbf{k}_i = \mathbf{k}_p$. For collinearly propagating waves this may be written $\omega_s n_s + \omega_i n_i = \omega_p n_p$, where n_m is the refractive index at frequency ω_m . Once the pump radiation is chosen, and thus ω_p fixed, then if the refractive indices at the signal, idler or pump frequencies are varied, the signal and idler frequencies generated in an OPO will tune. In laser pumped singly resonant OPO (SRO) only the signal (or idler) wave is resonated. In a doubly resonant OPO (DRO) both signal and idler waves are resonated.

Several pulsed OPO's were demonstrated that use LBO and KTP crystals as nonlinear media pumped by excimer lasers [1], mode-locked Nd:YAG laser [2], flash-pumped or diode-pumped Q-switched Nd:YAG lasers [3], [4], frequency

doubled Nd:YAG laser [5], frequency tripled Nd:YAG laser [6], frequency quadrupled Nd:YAG laser [7], frequency doubled all-solid state Q-switched Nd:YLF laser [8], frequency doubled mode-locked Nd:YLF lasers [9]–[11], mode-locked Ti:sapphire lasers [12]–[14], frequency doubled diode-pumped mode-locked Nd:YVO₄ laser [15].

The aim of this paper is to investigate the performance of a tunable pulsed DRO with LBO or KTP crystals, pumped by an electrooptically Q-switched frequency doubled Nd:YAG laser.

2. Theory

We consider an OPO with plane-parallel two mirror optical cavity. In the slowly varying envelope approximation, for collinear interaction of Gaussian waves along the z -axis, assuming no pump depletion and field absorption in the nonlinear material, the equations describing the parametric growth of the signal and idler field amplitudes E_s , E_i in the presence of a pump field amplitude E_p are [11], [16]:

$$\frac{dE_s}{dz} = j\kappa_s E_p E_i^* \exp(j\Delta kz), \quad (1a)$$

$$\frac{dE_i}{dz} = j\kappa_i E_p E_s^* \exp(j\Delta kz). \quad (1b)$$

Here, $\Delta k = k_p - k_s - k_i$ is the wave vector mismatch. The interaction coefficients κ_m ($m = s, i$) are given by $\kappa_m = \frac{\omega_m d_{\text{eff}}}{n_m c}$, where d_{eff} is the effective nonlinear coefficient, and c is the speed of light.

For a phase matched interaction ($\Delta k = 0$), the expressions for the signal and idler field amplitudes, after propagation through an effective gain interaction length l_g are given by:

$$E_s(l_g) = E_s(0) \cosh(\Gamma l_g) + j \frac{\kappa_s E_p}{\Gamma} E_i^*(0) \sinh(\Gamma l_g), \quad (2a)$$

$$E_i(l_g) = E_i(0) \cosh(\Gamma l_g) + j \frac{\kappa_i E_p}{\Gamma} E_s^*(0) \sinh(\Gamma l_g). \quad (2b)$$

The parametric amplitude gain Γ is given by

$$\Gamma = (\kappa_s \kappa_i |E_p|^2)^{1/2} = \left(\frac{2\omega_s \omega_i d_{\text{eff}}^2}{n_p n_s n_i \epsilon_0 c^3} I_p \right)^{1/2} \quad (3)$$

where $I_p = \frac{1}{2} n_p c \epsilon_0 |E_p|^2$ is the pump peak power density, and ϵ_0 is the permittivity of free space.

The oscillation threshold condition for a DRO is that the single pass parametric gain be sufficient to offset the round trip cavity losses α_s, α_i for both E field of

the signal and idler frequencies [17]

$$\frac{1}{1-\alpha_s} E_s(0) = E_s(0) \cosh(\Gamma l_g) + j \frac{\kappa_s E_p}{\Gamma} E_i^*(0) \sinh(\Gamma l_g), \quad (4a)$$

$$\frac{1}{1-\alpha_i} E_i(0) = E_s(0) \cosh(\Gamma l_g) + j \frac{\kappa_i E_p}{\Gamma} E_s^*(0) \sinh(\Gamma l_g). \quad (4b)$$

Taking the complex conjugate of (4b) and setting the determinant of the resulting two simultaneous equations to zero, we obtain the threshold condition:

$$\left(\cosh(\Gamma l_g) - \frac{1}{1-\alpha_s} \right) \left(\cosh(\Gamma l_g) - \frac{1}{1-\alpha_i} \right) - \sinh^2(\Gamma l_g) = 0, \quad (5)$$

$$\cosh(\Gamma l_g) = 1 + \frac{\alpha_s \alpha_i}{2 - \alpha_s - \alpha_i}.$$

For low loss resonators ($\alpha_s, \alpha_i \ll 1$) the oscillation threshold condition becomes

$$\Gamma^2 l_g^2 \simeq \alpha_s \alpha_i. \quad (6)$$

The threshold pump peak intensity I_p^{th} of a continuously operated (CW pumped) or synchronously pumped DRO (the length of the OPO optical cavity is adapted to the frequency of the ultrashort pulses generated by the pump mode-locked laser) results from (3) and (6).

In the case of OPO pumped with single pulse Q-switched lasers, the pump intensity is usually big enough to satisfy the threshold condition. The apparent threshold of the oscillator will be a pump power producing during pump pulse a sufficient gain for the oscillation to build out of the noise.

We have calculated the single pulse DRO threshold following the simplified model of BROSAN and BYER [16] for the pulsed SRO oscillation threshold with the assumptions:

– Gaussian time profile for the incident pump intensity which yields a time dependent gain coefficient Γ described by $\Gamma = T_0 \exp\left(-\frac{t^2}{\tau^2}\right)$, where τ is the $1/e^2$ intensity halfwidth of the pump pulse, and T_0 is the peak gain coefficient.

– Constant pump intensity during a single cavity transit ($\tau \gg \frac{n_p l_c}{c}$), where l_c is the nonlinear crystal length.

– Time independent gain profile of the width $\bar{\tau} = 2\tau$, and magnitude $\bar{\Gamma}$ given by $\bar{\Gamma} \simeq 1.34 T_0$.

For a single pulse pumped DRO, near degeneracy ($\lambda_s = \lambda_i$), assuming $\alpha_s = \alpha_i$, and the same signal and idler reflectance of the OPO mirrors, the equations for determining the apparent threshold become:

$$\sigma E_s(0) = E_s(0) \cosh(\bar{\Gamma} l_g) + j \frac{\kappa_s E_p}{\Gamma} E_i^*(0) \sinh(\bar{\Gamma} l_g), \quad (7a)$$

$$\sigma E_i(0) = E_i(0) \cosh(\bar{\Gamma}l_g) + j \frac{\kappa_i E_p}{\Gamma} E_s^*(0) \sinh(\bar{\Gamma}l_g) \quad (7b)$$

where: $\sigma = \frac{\exp(\beta)}{\sqrt{R_1 R_2 (1-\alpha)}}$; $\beta \simeq \frac{25L}{c\tau_p}$; L is the optical cavity length given by $L = L_0 + l_c(n_p - 1)$, with L_0 being the cavity physical length, τ_p is the FWHM pulse duration; R_1, R_2 are the signal (idler) reflectances of the OPO input and output mirrors; α is the round trip attenuation of the signal (idler) power in the nonlinear crystal. Taking the complex conjugate of (7b) and setting the determinant of the resulting two simultaneous equations to zero, we obtain the threshold pump peak intensity of a single pulse pumped DRO

$$I_p^{\text{th}}(\text{DRO}) = \frac{1.8 (\ln \sigma)^2}{\frac{8\pi^2 d_{\text{eff}}^2 g_s g_\lambda g_\alpha l_g^2 (1+\gamma)^2}{n_p n_s n_i \epsilon_0 c \lambda_s \lambda_i}} \quad (8)$$

where γ is the pump reflectance of the OPO output mirror; λ_s, λ_i are the signal and idler wavelengths; g_s is the signal spatial mode coupling coefficient [16] defined by $g_s = \frac{w_p^2}{w_p^2 + w_s^2}$, where w_p, w_s are the Gaussian mode electric field radii of pump and signal radiation beams; g_λ is the reduction factor in parametric gain that results from use of a pump of bandwidth $\Delta\lambda_p$ over that for a pump of negligible bandwidth [11]; g_α is the reduction in parametric gain from an ideal pumping with a collimated beam [11]; l_g is given by [16]: $l_g = l_w \operatorname{erf}\left(\frac{\sqrt{\pi} l_c}{2 l_w}\right)$, where l_w is the walk-off length $l_w = \frac{\sqrt{\pi} w_p}{2 \rho} \sqrt{\frac{w_p^2 + w_s^2}{w_p^2 + w_s^2/2}}$, ρ is the double refraction walk-off angle. The threshold power to noise power $\ln(P_m/P_0) \simeq 40$ was considered.

We calculated the signal (idler) spot size of DRO near degeneracy. Assuming a Gaussian profile for the electric fields, near degeneracy ($w_s \simeq w_i$), the driving polarization for the signal wave has the radius \bar{w}_s given by [11], [16]

$$\frac{1}{\bar{w}_s^2} = \frac{1}{w_s^2} + \frac{1}{w_p^2} \quad (9)$$

The radius of the signal (idler) polarization after a round trip through the optical cavity is

$$\bar{w}_{s1}^2 = \bar{w}_s^2 \left[1 + \left(\frac{2L\lambda_s}{\pi\bar{w}_s^2} \right)^2 \right] \quad (10)$$

By letting $\bar{w}'_s = w_s$ after several round trips, the steady state signal (idler) spot size is given by the following equations:

$$\left(\frac{\pi}{2L\lambda_s} \right)^2 \bar{w}_s^6 + \bar{w}_s^2 - w_p^2 = 0, \quad \frac{1}{w_s^2} = \frac{1}{\bar{w}_s^2} - \frac{1}{w_p^2} \quad (11)$$

The OPO frequency linewidth is given by [17]: $|\Delta f| \approx \frac{1}{bl_p}$, where $b = \frac{\partial k_i}{\partial \omega_i} - \frac{\partial k_s}{\partial \omega_s}$ is a dispersive parameter. The LBO is a crystal with small b , large tuning rate, and correspondingly with large parametric linewidth. The expression of the full half-power gain linewidth at signal (idler) wavelength is

$$\Delta\lambda_{s,i} = \frac{\lambda_{s,i}^2}{l_g} \frac{0.886}{\left| n(\lambda_s) - n(\lambda_i) - \lambda_s \frac{\partial n}{\partial \lambda} \Big|_{\lambda_s} + \lambda_i \frac{\partial n}{\partial \lambda} \Big|_{\lambda_i} \right|} \quad (12)$$

where $n(\lambda)$ is the refractive index given by Sellmeier equations.

3. Experimental results

The schematic diagram of the DRO optical cavity, formed by a pair of plane parallel mirrors is shown in Fig. 1.

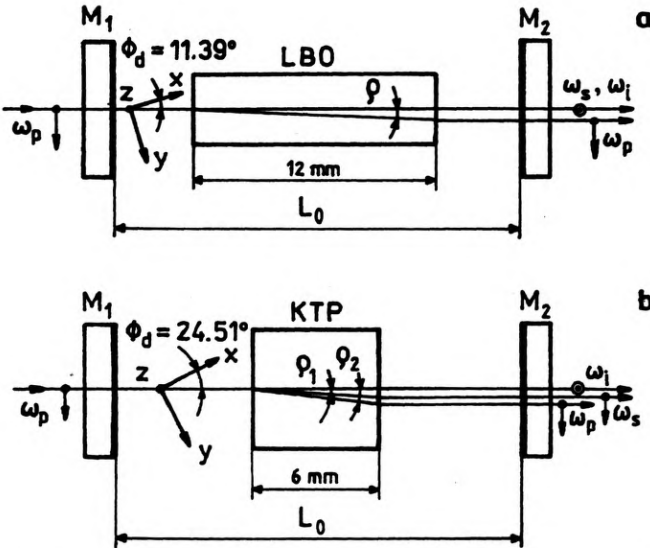


Fig. 1. Schematic diagram of the DRO optical cavity: a – LBO crystal, b – KTP crystal

The LBO crystal used in the present device is cut for type I phase matching ($e \rightarrow oo$) in the xy crystallographic plane, $\theta = 90^\circ$, $\phi = 10^\circ$, and was 12 mm in length with 4×4 mm aperture. The KTP crystal is cut for type II phase matching ($e \rightarrow oe$) in the xy crystallographic plane, $\theta = 90^\circ$, $\phi = 24.5^\circ$, and was 6 mm in length with 7×7 mm aperture. Both faces of LBO and KTP crystals are antireflection coated at 532/1064 nm. The pump laser is a non-focused frequency doubled Q-switched TEM₀₀ Nd:YAG laser amplifier, with pulse duration 10.5 ± 1 ns, and variable output pulse energy up to 50 mJ at 532 nm. This laser system has been described

elsewhere [18]. The main spectral characteristics of the OPO mirrors are:

- M_1 (input mirror) – high reflective (99.8%) at 1064 nm and > 99% over the range 930–1250 nm, 95% transmitting at 532 nm;
- M_2 (output mirror – 95% reflective at 1064 nm, 88–96% reflective over the range 930–1250 nm, 96% reflective at 532 nm.

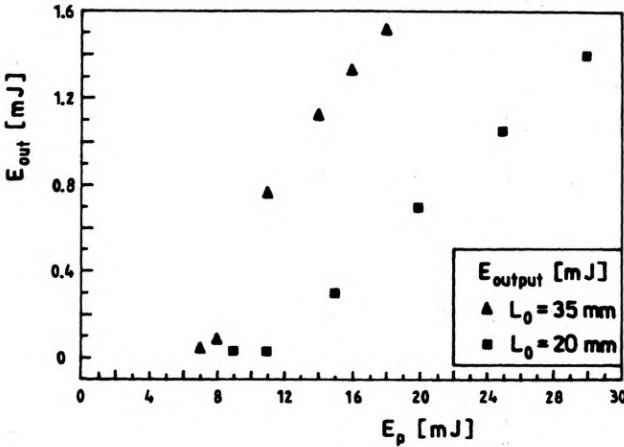


Fig. 2. Total output energy of the DRO-LBO as a function of pump energy

Due to the high reflectance at pump radiation of M_2 we obtained parametric gain on both forward and backward transmits through LBO and KTP crystals. The total output energy (signal and idler radiation) E_{out} of the DRO-LBO near degeneracy versus pump pulse energy E_p is shown in Fig. 2 for the cavity lengths $L_0 = 35$ mm and $L_0 = 20$ mm, respectively. The total output pulse energy near degeneracy is 1.51 mJ at 18 mJ pump energy. The highest total output efficiency of the DRO-LBO is 8.4%, the efficiency slope in the linear dependence range is about 13.8%.

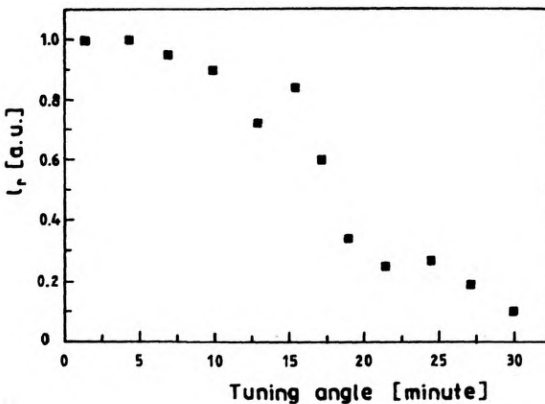


Fig. 3. Normalized DRO-LBO output energy of the signal and idler radiation versus tuning angle from degeneracy

We observed the parametric oscillation threshold at 10 mJ pump energy, corresponding to a peak power density of 44 MW/cm² on the LBO input face, for $L_0 = 35$ mm, and 7 mJ, 29 MW/cm², for $L_0 = 20$ mm. The level of the pump intensity is restricted by the damage of M_1 . Using Eq. (8) we calculated the apparent oscillation threshold $I_p^{\text{th}}(\text{DRO-LBO}) = 16$ MW/cm² for $L_0 = 35$ mm, and 9 MW/cm² for $L_0 = 20$ mm.

The parameters used for DRO threshold calculation are: $L = 43$ mm (28 mm), $\alpha = 0.06$, $R_1 = 1$, $R_2 = 0.95$, $\gamma = 0.9$, $l_g = 11.9$ mm [18], $n_p = n_s = n_i = 1.6055$, $\epsilon_0 = 8.854 \times 10^{-12}$ F/m, $c = 3 \times 10^8$ m/s, $d_{\text{eff}} = 0.82 \times 10^{-12}$ m/V [19], $g_s = 0.92$, $g_\lambda = 0.97$ ($\Delta\lambda = 1.55$ nm [18], $\Delta\lambda_p = 0.33$ nm), $g_\alpha = 1$, $\tau_p = 11$ ns.

The tuning of the OPO was achieved by rotation of the LBO crystal in the xy crystallographic plane. The output signal and idler energy, measured at fixed pump energy, decreases with the rotation of the LBO crystal from the degeneracy angle, as shown in Fig. 3. I_r is the output energy normalized to the degeneracy output energy level. This result and the following ones were obtained with a pump pulse energy of 15 mJ (a factor of ~ 1.5 above threshold).

The calculated radii of the signal (idler) wave near degeneracy, as results from (11), are $w_s = 0.32$ mm ($L_0 = 35$ mm) and $w_s = 0.275$ mm ($L_0 = 20$ mm), being significantly less than the radius of the Gaussian pump wave $w_p = 1.1$ mm on LBO crystal. The calculated full divergence angle of a corresponding Gaussian signal (idler) beam is $\theta_s = 2\lambda_s/\pi w_s \simeq 2.12$ mrad, which is in good agreement with the experimentally measured signal spot of 5 mm at a distance of ~ 2 m from the OPO output mirror.

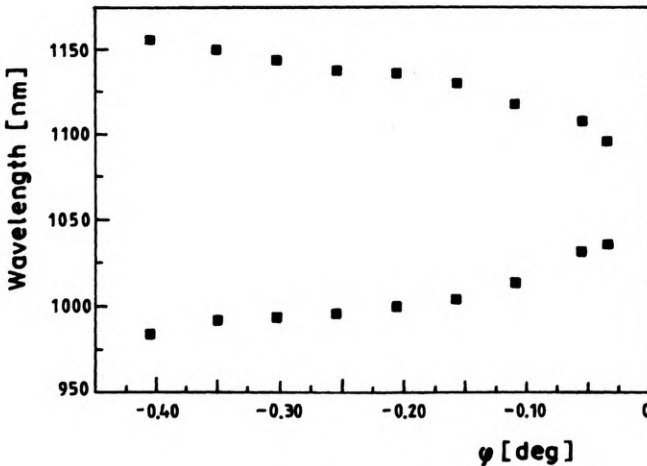


Fig. 4. Angle-tuning data for DRO-LBO

The wavelength of the signal and idler waves versus tuning angle were measured over the tuning range. Figure 4 shows the tuning characteristics versus the incident angle φ of the pump radiation on the input surface of the LBO crystal ($\varphi = 0$ at

degeneracy). Using the Sellmeier equations for LBO crystals we calculated the internal angle of degeneracy $\Phi_d(\text{LBO}) \approx 11.39^\circ$. The DRO-LBO was continuously tuned from 970 nm to 1175 nm by tilting the LBO crystal with 0.4° from the degeneracy orientation.

The spectrum of the frequency doubled Nd:YAG laser and the OPO emission spectrum for signal and idler radiation were taken by use of a grating monochromator with a resolution better than 0.1 nm, and were averaged over a train of pump pulses. Figure 5 shows the relative intensity I_s (in arb. units) of the frequency doubled Nd:YAG laser radiation versus wavelength. The bandwidth of the pump laser is about 0.3 nm.

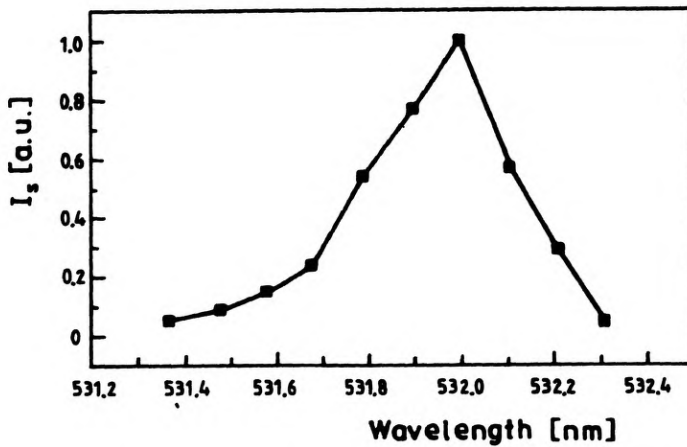


Fig. 5. Spectrum of frequency doubled Nd:YAG laser radiation

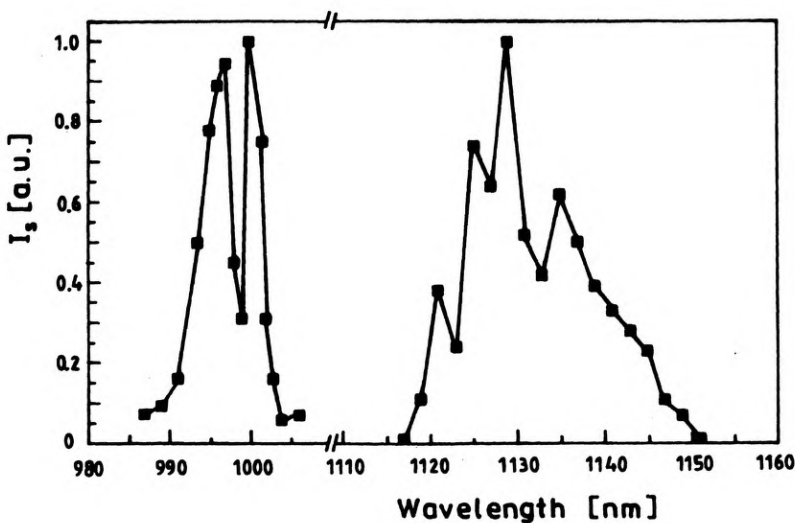


Fig. 6. Spectrum of DRO-LBO

Figure 6 shows the relative intensity I_s (in arb. units) of the signal and idler radiation versus wavelength, for a fixed orientation of the LBO crystal. We observed a double structure for each spectrum, probably due to the "cluster effect" characteristic of DRO's. The FWHM linewidth of the signal wave with 998 nm central wavelengths was ~ 10 nm, and ~ 13 nm for the corresponding idler wave with 1136 nm wavelength, as shown in Fig. 6. The linewidths calculated by (12) at $\lambda_s = 998$ nm ($\lambda_i = 1136$ nm), and $\lambda_s = 900$ nm ($\lambda_i = 1301$ nm) were $\Delta\lambda_s = 32$ nm ($\Delta\lambda_i = 41$ nm), and $\Delta\lambda_s = 9$ nm ($\Delta\lambda_i = 19$ nm), respectively. Expression (12) gives correct results if the shift of the central wavelength of the signal (idler) line from the degeneracy wavelength is much larger than the signal (idler) linewidth.

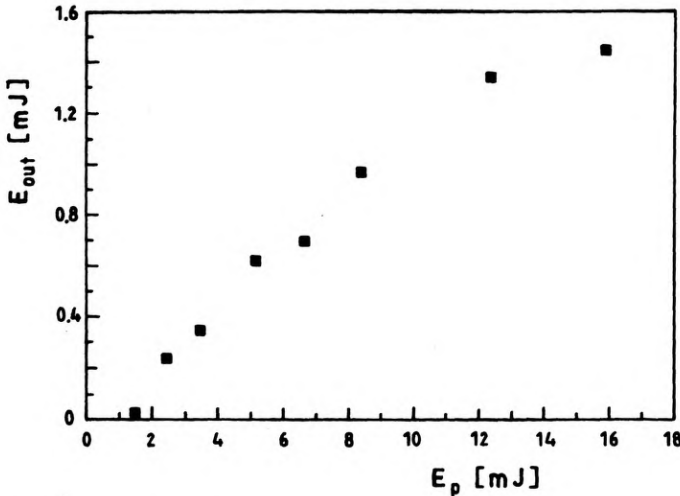


Fig. 7. Total output energy of DRO-KTP as a function of pump energy

The oscillation threshold for pulse pumped DRO with KTP, calculated by relation (8), is $I_p^{th}(\text{DRO-KTP}) = 2.5$ MW/cm². The parameters for the DRO-KTP threshold calculation are: $L = 24.7$ mm ($L_0 = 20$ mm), $\alpha = 0.06$, $R_1 = 1$, $R_2 = 0.95$, $\gamma = 0.9$, $l_g = 5.9$ mm, $n_p = 1.7868$, $n_s = 1.7453$, $n_i = 1.8297$, $\epsilon_0 = 8.854 \times 10^{-12}$ F/m, $c = 3 \times 10^8$ m/s, $d_{eff} = 3.18 \times 10^{-12}$ m/V [19], $g_s = 0.94$, $g_i = 0.93$, $g_a = 1$, $\tau_p = 11$ ns.

We observed experimentally the oscillation threshold at a pump threshold energy $E_{pt} \approx 1.5$ mJ, corresponding to a peak intensity of 5.7 MW/cm² on the KTP input face. Output energy of 1.45 mJ has been obtained with 16 mJ pump energy (Fig. 7). The highest total output efficiency of the DRO-KTP is 9.1%, the efficiency slope in the linear dependence range is 11.9%.

At pump energy over 9 mJ, once the factor above threshold E_p/E_{pt} exceeds its optimum value, we observe a decrease in the energy conversion efficiency of the pump radiation E_p into the signal and idler radiation E_s . This behaviour was studied for the first time for plane-waves by SIEGMAN [20], and then carried out by Bjorkholm for beams having Gaussian intensity profiles [21]. For uniform plane-

wave pumping total pump depletion and 100 percent conversion efficiency could be obtained, whereas the maximum possible conversion efficiency for Gaussian beams is reduced from unity to ~ 0.7 [4]. The energy conversion efficiency is less than the peak-power conversion efficiency due to the shorter duration of the signal and idler radiation in comparison with the pump radiation.

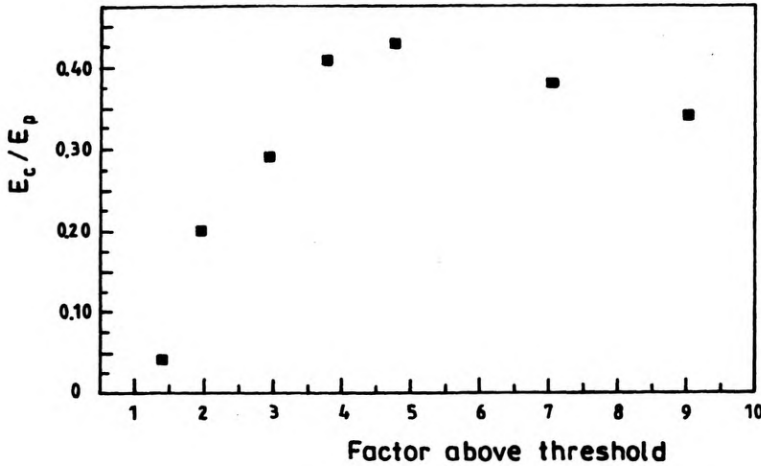


Fig. 8. Dependence of the pump conversion efficiency in DRO-KTP on the factor above threshold (E_p/E_{pt})

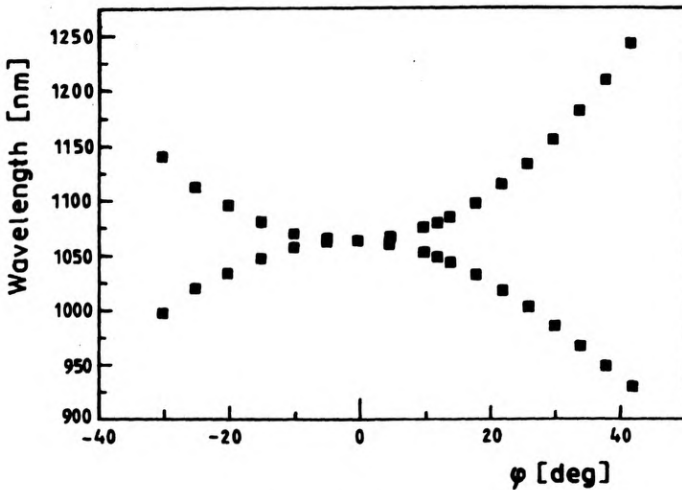


Fig. 9. Angle-tuning data for DRO-KTP

The maximum energy conversion efficiency measured experimentally for DRO-KTP was 43% at a factor ~ 5 above threshold (Fig. 8).

The signal (idler) wavelengths of the DRO depending on the external tuning angle ϕ of the KTP crystal are plotted in Fig. 9 ($\phi = 0$ at degeneracy). The calculated

internal angle at degeneracy for the KTP crystal is $\Phi_d(\text{KTP}) \simeq 24.51^\circ$. The range of tunability was from 930 nm to 1243 nm by rotating the KTP crystal at 42° from the degeneracy orientation.

The signal (idler) radiation linewidth of the DRO-KTP given by Eq. (12) is ~ 1 nm near degeneracy. The experimentally measured linewidths are 0.65 nm for the signal radiation ($\lambda_s = 1052.6$ nm) and 0.8 nm for the idler radiation ($\lambda_i = 1075.5$ nm), respectively (Fig. 10).

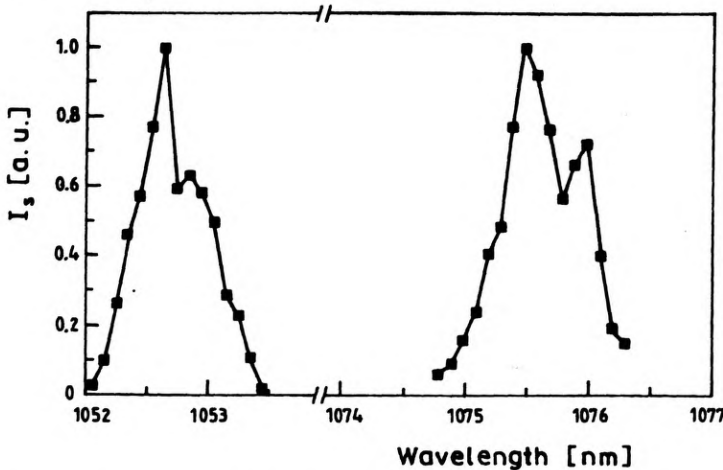


Fig. 10. Spectrum of DRO-KTP

Even though the LBO crystal used in our experiments is twice longer than the KTP crystal, the oscillation threshold for KTP is lower mainly because of the higher effective nonlinear coefficient. The LBO crystal has a larger tuning rate, but also correspondingly a larger linewidth in comparison with the KTP crystal. The linewidth of the DRO with KTP crystal is less than 1 nm as compared to more than 10 nm for LBO. The tuning angle for KTP is more than an order of magnitude higher than for LBO, at the same range of wavelength tunability.

4. Conclusions

We have conducted a comparative study of LBO and KTP crystals as nonlinear materials for DRO's pumped by the second harmonic of a nanosecond Nd:YAG laser. We have deduced analytical expressions of the pump peak power density at the oscillation threshold for single pulse pumped DRO, signal (idler) wave spot size, and signal (idler) linewidth.

The experimentally measured thresholds for OPO optical cavity of 20 mm in length are 29 MW/cm^2 for LBO crystal, and 6 MW/cm^2 for KTP crystal.

The tuning from 970 to 1175 nm is obtained for the DRO-LBO, corresponding to an external tuning angle of 0.4° , and from 930 to 1243 nm for the DRO-KTP, corresponding to an external tuning angle of 42° .

The linewidths of the signal (idler) radiation emitted by DRO-LBO at 998 nm (1136 nm) wavelength were 10 nm (13 nm) and 0.65 nm (0.8 nm) at 1052.6 nm (1075.5 nm) for DRO-KTP.

References

- [1] ROBERTSON G., HENDERSON A., DUNN M. H., *Appl. Phys. Lett.* **60** (1992), 271.
- [2] CHUNG J., SIEGMAN A. E., *J. Opt. Soc. Am. B* **10** (1993), 2201.
- [3] KATO K., *IEEE J. Quantum Electron.* **27** (1991), 1137.
- [4] MARSHALL L. R., KAZ A., *J. Opt. Soc. Am. B* **10** (1993), 1730.
- [5] KATO K. *IEEE J. Quantum Electron.* **26** (1990), 2043.
- [6] HANSON F., DICK D., *Opt. Lett.* **16** (1991), 205.
- [7] TANG Y., CUI Y., DUNN M. H., *Opt. Lett.* **17** (1992), 192.
- [8] HALL G. J., FERGUSON A. I., *Opt. Lett.* **18** (1993), 1511.
- [9] GRASSER C., WANG D., BEIGANG R., WALLENSTEIN R., *J. Opt. Soc. Am. B* **10** (1993), 2218.
- [10] CHEN P. L., WANG Y., LIU J. M., *J. Opt. Soc. Am. B* **12** (1995), 2192.
- [11] MC CARTHY M. J., HANNA D. C., *J. Opt. Soc. Am. B* **10** (1993), 2180.
- [12] EBRAHIMZADEH M., FRENCH S., MILLER A., *J. Opt. Soc. Am. B* **12** (1995), 2180.
- [13] NEBEL A., FALLNICH C., BEIGANG R., WALLENSTEIN R., *J. Opt. Soc. Am. B* **10** (1993), 2195.
- [14] HACHE A., ALLAN G. R., VAN DRIEL H. M., *J. Opt. Soc. Am. B* **12** (1995), 2209.
- [15] KAFKA J. D., WATTS M. L., PIETERSE J. W., *J. Opt. Soc. Am. B* **12** (1995), 2147.
- [16] BROSANAN S. J., BYER R. L., *IEEE J. Quantum Electron.* **15** (1979), 415.
- [17] HARRIS S. E., *Proc. IEEE* **57** (1969), 2096.
- [18] DABU R., FENIC C., STRATAN A., MUSCALU L., *Opt. Appl.* **26** (1996), 171.
- [19] VELSKO S. P., WEBB M., DAVIS L., HUANG C., *IEEE J. Quantum Electron.* **27** (1991), 2182.
- [20] SIEGMAN A. E., *Appl. Opt.* **1** (1962), 739.
- [21] BJORKHOLM J. E., *IEEE J. Quantum Electron.* **7** (1971), 109.

*Received May 19, 1998
in revised form August 3, 1998*